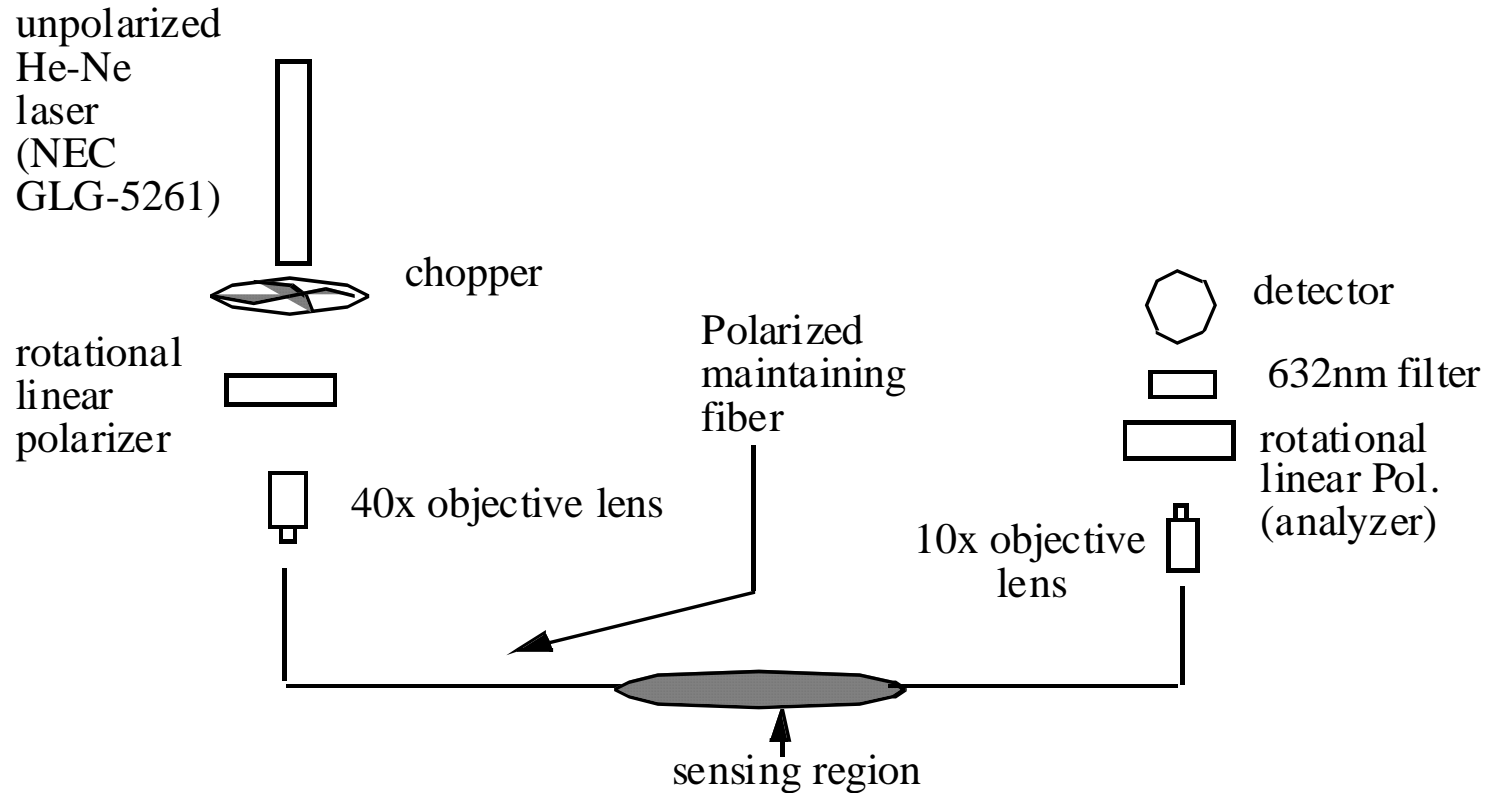


Other Types of Sensors

Wei-Chih Wang

Southern Taiwan University of
Technology

Polarmetric Strain Sensor



Polarimetric Sensor

The birefringence property arising from optical anisotropy is used in the study of photoelastic behaviour. The anisotropy may be due to naturally occurring crystalline properties or due to stress induced birefringence. It is the latter that is used in a photoelastic fiber optic strain gauge. In a simple setup two lead fibers are used to illuminate and collect light passing through a photoelastic specimen. A pair of linear polarizers is used in the crossed form to obtain a conventional polariscope. In such a case the intensity at each point on the specimen is given by

$$I = I_0 \sin^2 2\theta \sin^2 \frac{\alpha'}{2}$$

where I_0 is the total light intensity and θ is the angle that the principal stress directions make with respect to the axes of the polarisers.

Due to stress birefringence the orthogonally polarized light waves travel with a phase difference α given by

$$\alpha = \frac{2\pi}{\lambda} (n_1 - n_2) d = \frac{2\pi}{f_a} (\sigma_1 - \sigma_2) d$$

where λ is wave length, n is the index of refraction, d is the thickness in the direction of light propagation, C is stress-optic coefficient and $f_a = (\lambda \setminus C)$ is known as material fringe value.

When the polarisers are oriented 45^0 w.r.t. principal stress directions equations (28) and (29) simplify to

$$I = I_0 \sin^2 \frac{\alpha'}{2}$$

with $\alpha = (2\pi /fa) \sigma d$ where the applied load is assumed to produce a uniaxial stress . By taking the derivative of the above equation we obtain

$$\Delta I = I_0 \Delta \left(\frac{\alpha'}{2} \right) \sin \alpha'$$

Fiber optic Magnetic Sensors

Current Technology:

Low Frequency ($< 10\text{Hz}$, $< 10^{-9}\text{T}$ or 10^{-5}G)

fluxgates

superconducting quantum interference device

stress-driven magnetoelastic devices

High frequency ($> 10\text{Hz}$)

wire loop

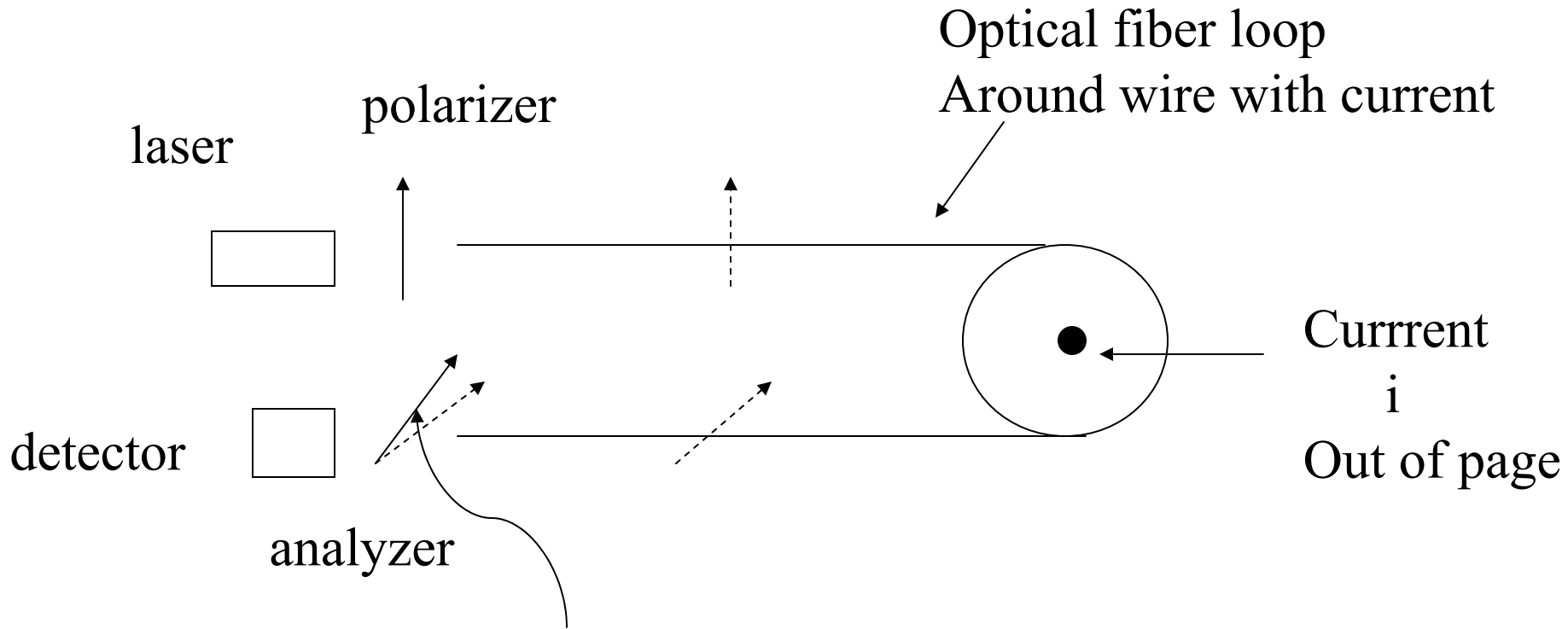
fiber optic Faraday devices

bulk optic faraday devices

Electrical current and magnetic sensors

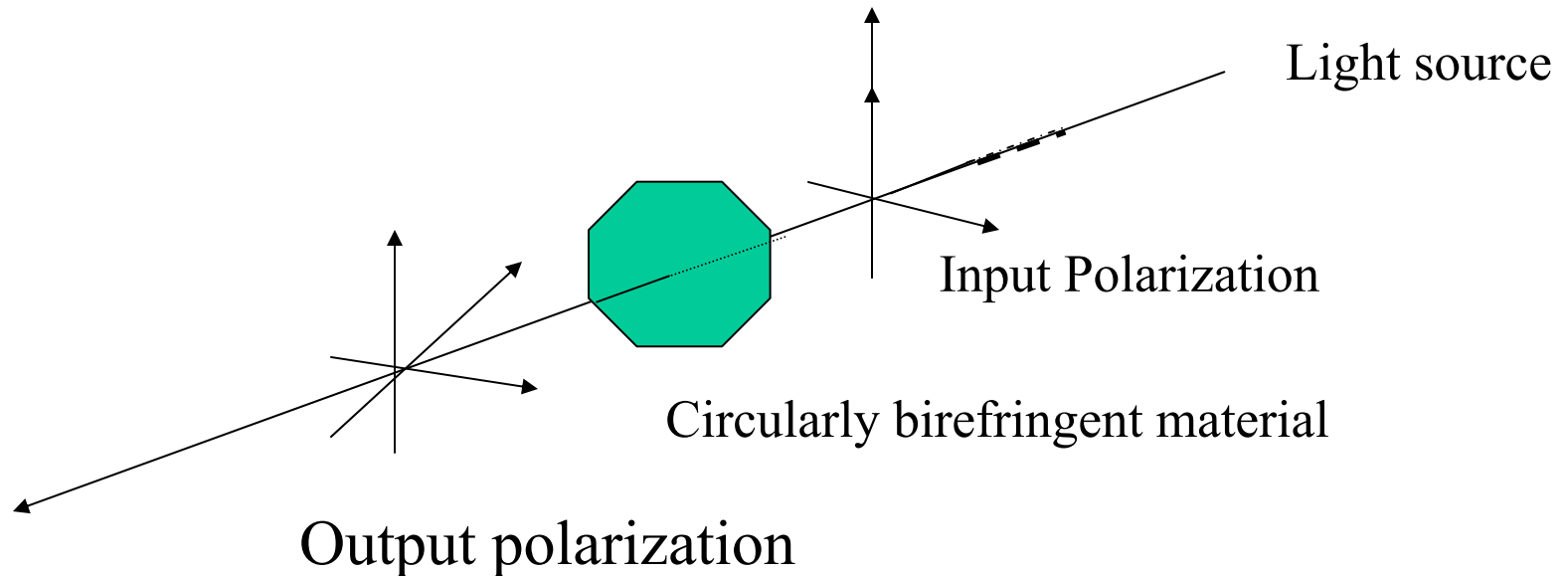
- Electrical current sensor
 - fiber is wound around quartz crystals and the resulting piezoelectric induced stress in the fiber is monitored with a white-light interferometer. Voltages from 0.1 to 1600 V are measured with errors well below 1% and maximum detectable current is >23kA with 2A resolution (ABB Corporate Research Center)
 - electrostrictive transducer made from lead-titanate-doped magnesium niobate with about 65 meters of fiber wrapped around it. Voltage sensitivity as low as 20 nV/ has been reported (Fabiny, Vohra, and Bucholtz 1994).

Polarimeter



θ Angle of rotation due to birefringent effect in fiber

Faraday Effect Sensors



Rotation of plane of polarization by circularly birefringent medium

Faraday Effect in optical fiber (current sensor)

In the presence of a magnetic field H ,
Circularly birefringence induced in the fiber will rotate the plane of polarization of linearly polarized light by an angle of θ

$$\theta = V \int (H dl)$$

Where V is the strength of the Faraday effect in fiber (function of optical wavelength and composition)

In current sensing configuration, fiber is wrapped N times around a conductor carrying current I . Using Ampere law, the line integral of the magnetic field reduces to

$$\theta = V Ni$$

Power at detector if azimuth of the analyzer is set at $\pm 45^\circ$:

$$P = P_0/2 (1 \pm \sin 2\theta)$$

Where $P_0/2$ is the average intensity at the detector. For small current

$$P = P_0/2 (1 + 2VNi)$$

The intensity is a linear function of current, $V = 4.6 \times 10^{-6}$ rad/A
independent of radius of fiber coil

Coiling fiber around a conductor produce a compact sensor whose geometry takes advantage of the symmetry of the field due to the current. However, bending of fiber introduces stress in the fiber, which in turn induces linear birefringence β_b given by

$$\beta_b = K_\lambda \left(\frac{r}{\rho}\right)^2$$

Where r is radius of the fiber cross section ρ is radius of the fiber coil, K_λ is a material parameter having value of 1.3×10^6 rad/m for silica fiber at $\lambda = 630$ nm.

In the presence of **linear birefringence (due to stress and intrinsic)**, the intensity equation becomes

$$P = \frac{P_o}{2} \left(1 + \frac{\alpha_F}{\gamma} \sin \gamma L \right)$$

Where $\gamma^2 = \beta^2 + \alpha_F^2$ and $\beta = \beta_i + \beta_b$ includes the intrinsic and Stress induced birefringence β_i of fiber and β_b . The **circular birefringence due to the Faraday effect is** written as $\alpha_F = 2\theta/L$ where $L = 2\pi N\rho$

the intensity equation becomes

$$P = \frac{P_o}{2} \left(1 + \frac{\alpha_F}{\sqrt{(\beta_i + \beta_b)^2 + \alpha_F^2}} \sin \sqrt{(\beta_i + \beta_b)^2 + \alpha_F^2} L \right)$$

$$= \frac{P_o}{2} \left[1 + \left(2 \frac{V}{\beta L} \sin \beta L \right) Ni \right] = \frac{P_o}{2} [1 + V_{eff} Ni]$$

$$\alpha_F = 2\theta/L = 2VNi/L \quad \text{where } L = 2\pi N\rho \text{ and } \theta = Vni$$

1. $\beta L \gg 1$, $V_{eff} \ll V$ *verdet constant has been quenched by linear birefringence*
2. $\beta L = n\pi \Rightarrow$ *immune to faraday effect* $\sin \beta L = -1$

Problems are resolved by

1. Twisting the fiber, annealing the fiber and used circularly birefringence fibers
2. Built-in circularly birefringence fibers: helical-core fiber, spun fiber and elliptical fiber, birefringence fiber

Twisting fiber

Putting a twist of ξ radians per meter onto an optical fiber induces fixed circular birefringence at

$$\alpha_t = g\xi$$

$\xi=0.13$ to 0.16 for silica fiber at $\lambda =630\text{nm}$

If $\alpha_t \gg \beta \gg \alpha_F$ then $\gamma \sim \alpha_t(1 + \beta^2 / 2\alpha_t^2)$

$$P = \frac{P_o}{2} \left(1 + \frac{\alpha_F}{\gamma} \sin \gamma L\right) = \left(1 + \frac{\alpha_F}{\sqrt{(\beta_i + \beta_b)^2 + \alpha_F^2}} \sin \sqrt{(\beta_i + \beta_b)^2 + \alpha_F^2} L\right)$$

$$= \frac{P_o}{2} \left(1 + \frac{\alpha_F}{\alpha_t(1 + \beta^2 / 2\alpha_t^2)} \sin(\alpha_t(1 + \beta^2 / 2\alpha_t^2)L)\right) \quad q = 1 - (\beta^2 / 2\alpha_t^2)$$

$$= \frac{P_o}{2} (1 + q \sin(\alpha_t + 2VNi)) = \frac{P_o}{2} (1 + (1 - (\beta^2 / 2\alpha_t^2)) \sin(\alpha_t + 2VNi))$$

(equation only works for untwisted set (twisted but set))

$$= \frac{P_o}{2} (1 + 2qVNi) \quad (\text{twisted but set } P=P_o/2 \text{ when } i=0)$$

sensors

- Electrical current sensor
 - fiber is wound around quartz crystals and the resulting piezoelectric induced stress in the fiber is monitored with a white-light interferometer. Voltages from 0.1 to 1600 V are measured with errors well below 1% and maximum detectable current is >23kA with 2A resolution (ABB Corporate Research Center)
 - electrostrictive transducer made from lead-titanate-doped magnesium niobate with about 65 meters of fiber wrapped around it. Voltage sensitivity as low as 20 nV/ has been reported (Fabiny, Vohra, and Bucholtz 1994).

Polarimetric Glucose Sensor

- Polarimetric measurement of glucose concentration is based on optical rotatory dispersion (ORD) a phenomenon by which a solution containing a chiral molecule rotates the plane of polarization for linearly polarized light passing through it.

Polarimetric Glucose Sensor

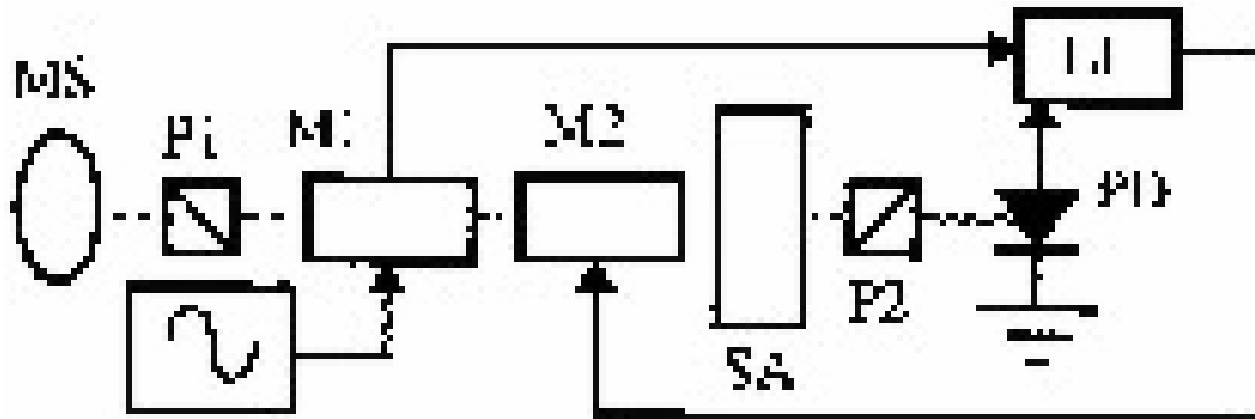
- The rotation is the result of a difference in refractive indices n_L and n_R for left and right circularly polarized light traveling through the electron cloud of a molecule.

Polarimetric Glucose Sensor

- The signal produced by the detector is proportional to the square of the E-field of the light incident on it and is given by:

$$I \propto E^2 = E_0^2 \sin^2[\theta \sin(\omega t) + \varphi] = E_0^2 \left\{ \frac{1}{2} \theta^2 + \varphi^2 - \frac{1}{2} \theta^2 \cos(2\omega t) + 2\theta\varphi \sin(\omega t) \right\}$$

Optical Setup



By Roger J. McNichols

Bragg Grating Sensor

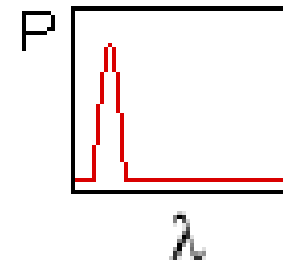
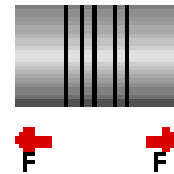
- **Features**
- Bragg Gratings have low insertion losses and are compatible with existing optical fibers used in telecommunication networks.
- Bragg Gratings allow low-cost manufacturing of very high quality wavelength-selective optical devices.
- Phase masks used to photo-imprint the Gratings allow manufacturing that is relatively simple, flexible, low-cost and large-volume.

Bragg Grating Sensor

Bragg grating based sensor system is to monitor the shift in wavelength of the returned bragg signal with the changes in the measurand (in this case strain). The bragg wavelength or resonance condition of a grating is given by

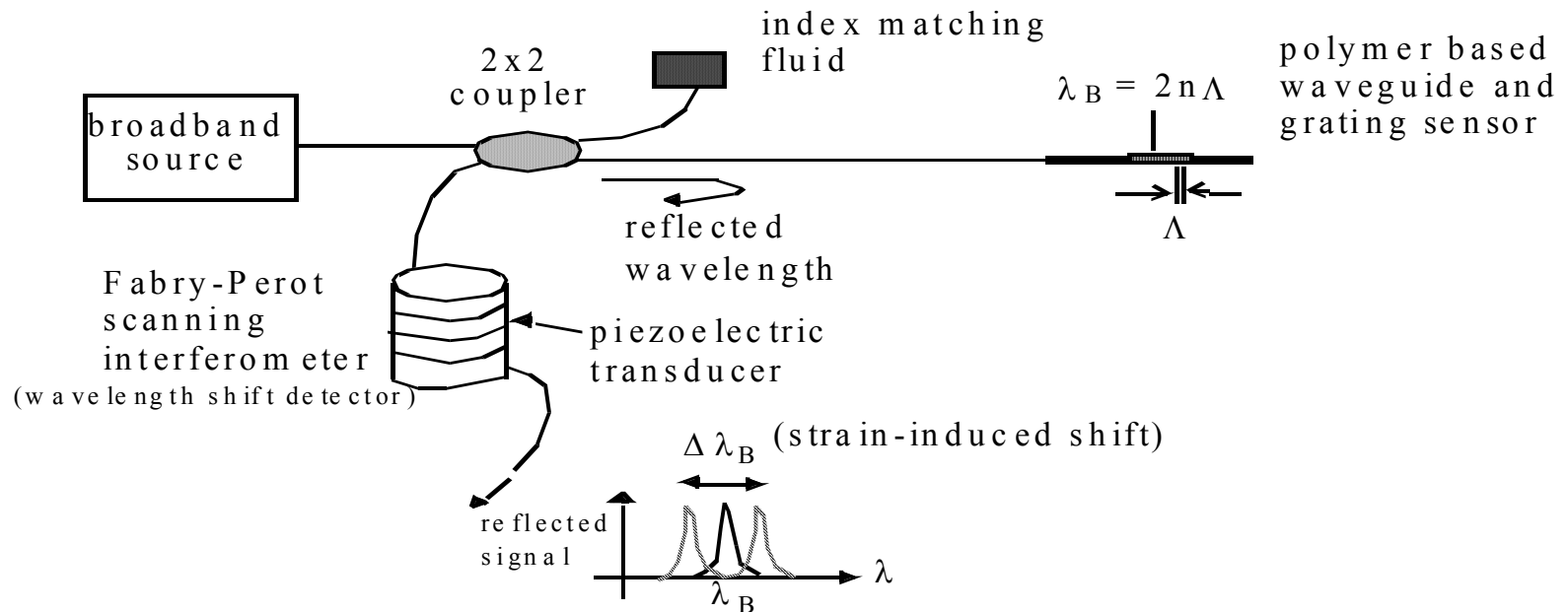
$$\lambda_B = 2n\Lambda$$

Where Λ is the grating pitch and n is the effective index of the core.



Bragg Grating Sensors

The Bragg bandwidth of the reflected by the grating. The bandwidth of the reflected signal depends on several parameters, particularly the grating length. Perturbation of the grating results in a shift in the Bragg wavelength of device which can be detected in either the reflected or transmitted spectrum.



Strain and Temperature Sensing

$$\Delta\lambda_B = 2n\Lambda\left[\varepsilon_{zz}\left(1 - \left(\frac{n^2}{2}\right)(\rho_{12} - \nu(\rho_{11} + \rho_{12}))\right)\right] + \left(\alpha + \frac{\left(\frac{dn}{dT}\right)}{n}\right)\Delta T$$

Where ρ_{ij} are Pockel's coefficients of the stress-optic tensor, ν is poisson's ratio, ε_{zz} is the longitudinal strain and α is the coefficient of thermal expansion of the waveguide, and ΔT is the temperature change. It is not possible to separate the effect of the temperature from the effect of the strain with only one sensor.

Strain and Temperature Sensing

Strain response due to

- Physical change corresponding to pitch change in grating
- index change due to photoelastic effect

Thermal response arise from

- Internal thermal expansion
- temperature dependent index change

Strain Sensing

For silica core fiber under constant temperature, the strain response is

$$\frac{1}{\lambda_B} \frac{\delta\lambda_B}{\delta\varepsilon} = 0.78 \times 10^{-6} \mu\varepsilon^{-1}$$

The response is 1nm per 1000 $\mu\varepsilon$ at 1.3 μm

Temperature Sensing

In silica fiber, thermal effect is dominated by $\delta n/\delta T$, which account for 95% of the shift. The normalized thermal response at constant strain is therefore,

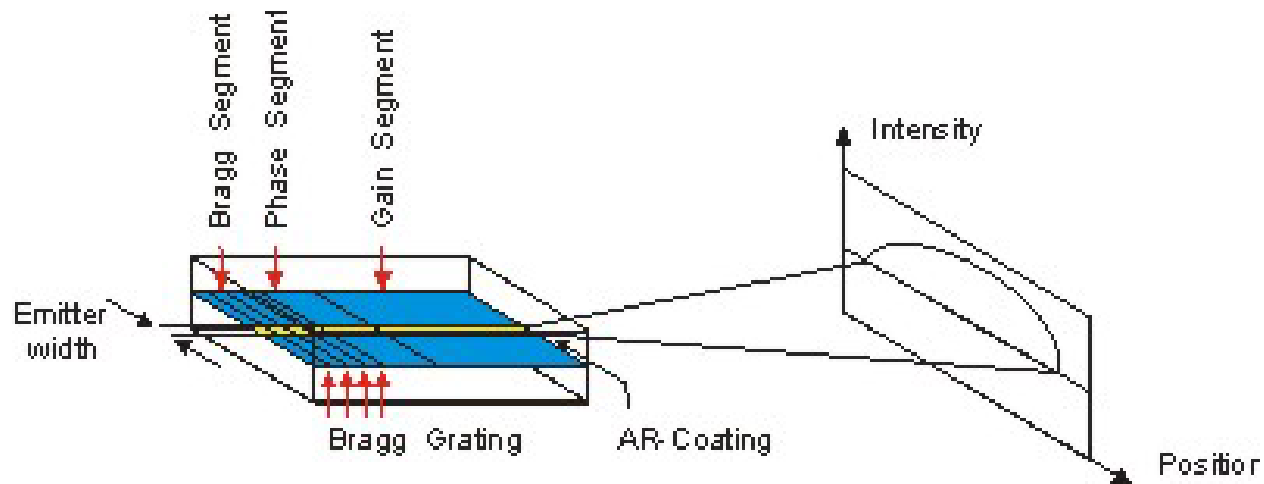
$$\frac{1}{\lambda_B} \frac{\delta \lambda_B}{\delta T} = 6.67 \times 10^{-6} \text{ } ^\circ\text{C}^{-1}$$

1pn is requires to resolve temperature change of 0.1°C

Bragg Grating Sensor

- **Applications**
- Bragg Gratings have proven attractive in a wide variety of optical fiber applications, such as:
 - Narrowband and broadband tunable filters
 - Optical fiber mode converters
 - Wavelength selective filters, multiplexers, and add/drop Mach-Zehnders
 - Dispersion compensation in long-distance telecommunication networks
 - Gain equalization and improved pump efficiency in erbium-doped fiber amplifiers
 - Spectrum analyzers
 - Specialized narrowband lasers
 - Optical strain gauges in bridges, building structures, elevators, reactors, composites, mines and smart structures

Distributive feedback laser



Sacher Lasertechnik Group.

Using grating to select the desired operating wavelength

Surface Plasmon Resonator Sensor

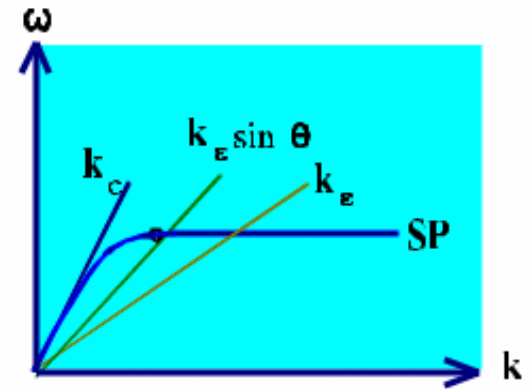
Surface plasmon resonance sensor use surface plasma waves to probe bimolecular interactions occurring at the surface of a sensor.

SPR Theory

According to Maxwell's theory, surface Plasmons can propagate along a metallic Surface and have a spectrum of eigen frequencies ω related to the wave-vector (k) by a dispersion relation,

$$k_{SP} = \sqrt{\frac{\epsilon_1 \epsilon_2}{\epsilon_1 + \epsilon_2}}$$

Where $\epsilon_2 = \epsilon_2' + j\epsilon_2''$ and ϵ_1 are dielectric constants of metal and the medium in contact with it.



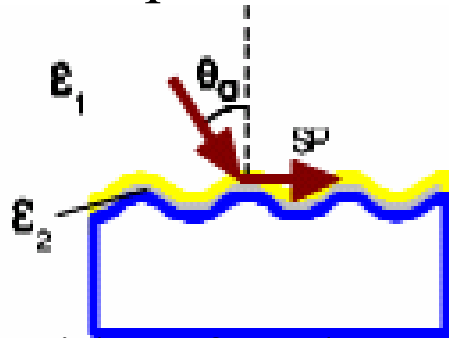
Wave vector of light at frequency ω traveling through the Medium ϵ_1 is described by:

$$\mathbf{k}_1 = \frac{\omega}{c} \sqrt{\epsilon_1}$$

If ϵ_1 is air, the SP's dispersion relation never intersect with the dispersion relation of light in air ($k=\omega/c$), they cannot be excited directly by a freely propagating beam of light incident upon the metal surface

Excite Plasmons via a Grating Coupler

If grating constant b , the light wave vector is increased by an Additional term $2\pi/b$, and the SP's dispersion relation can be matched by light vector parallel to the surface

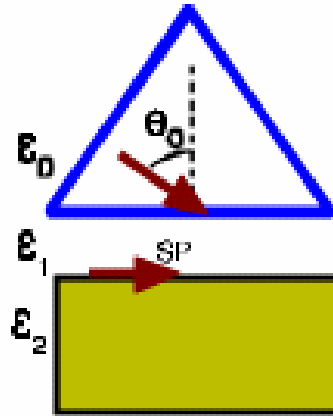


For an angle of incident θ_0 , the resonance condition is

$$\frac{\omega}{c} \sin \theta_0 + \frac{2\pi}{b} = \frac{\omega}{c} \sqrt{\frac{\epsilon_2}{\epsilon_2 + 1}}$$

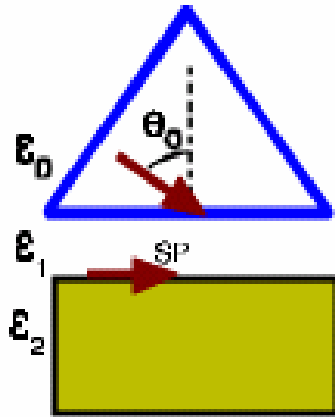
The resonance can be observed at angle θ_0 as minimum reflected intensity

Prism coupling Method



The concept is based on the fact that the light line can be lowered by a factor $\epsilon_0^{0.5}$ if the beam is traveling through an optical denser medium. Plasmons can be excited by TM polarized light undergoing total internal reflection on prism surface where evanescent wave penetrates to metal/air interface

Prism coupling introduced by Otto

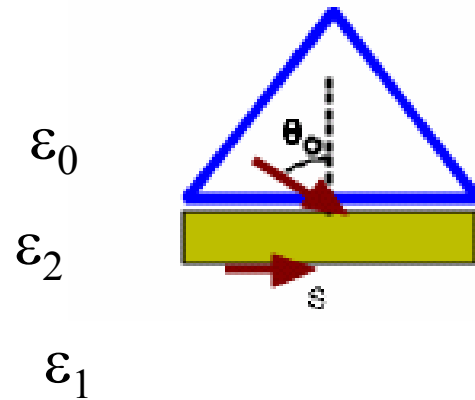


Metal surface is separated from the Prism by an additional layer (air slit), ϵ_1 . SP resonance occurs at metal-dielectric interface.

For an angle of incident θ_o , the resonance condition is

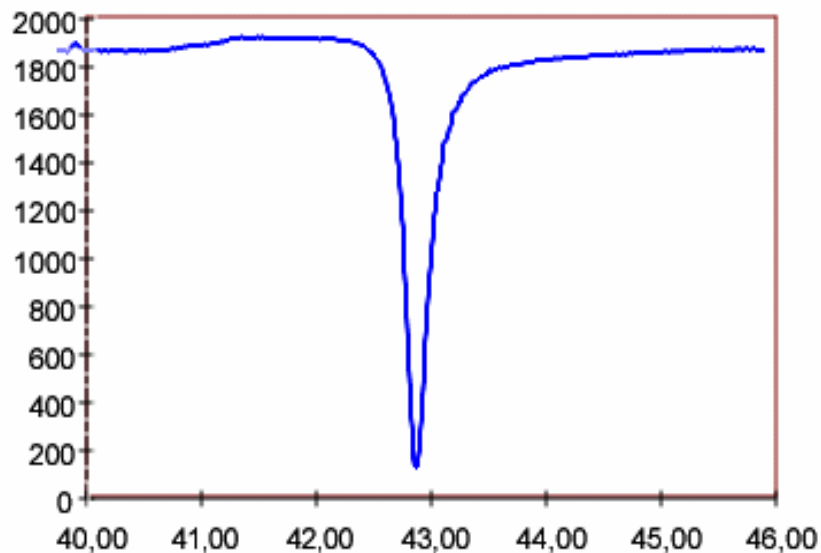
$$\frac{\omega}{c} \sqrt{\epsilon_0} \sin \theta_o = \frac{\omega}{c} \sqrt{\frac{\epsilon_1 \epsilon_2}{\epsilon_1 + \epsilon_2}}$$

Kretschmann Configuration



Metallic layer is formed on the prism surface and acts as the spacer. for the correct film thickness, the evanescent field expanding through the metal may couple to the SP on the opposite (ϵ_2/ϵ_1) metal surface.

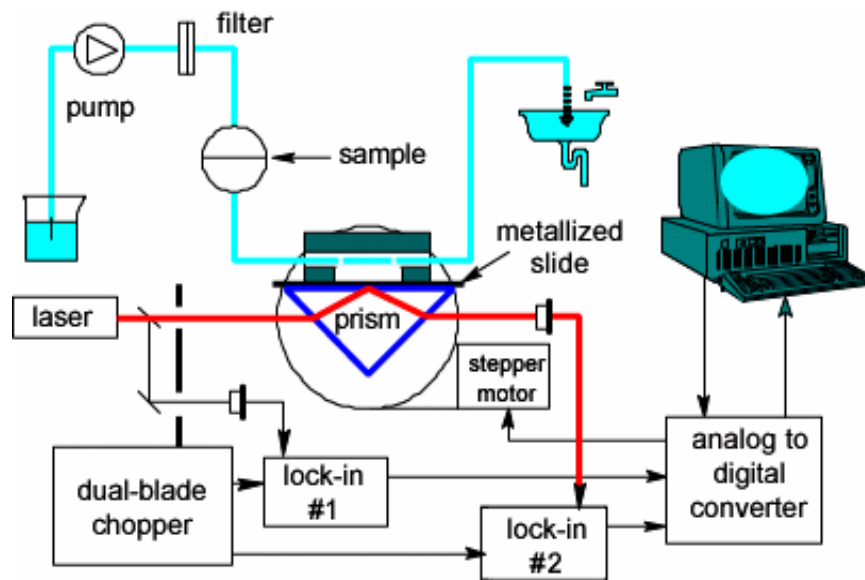
Reflected Intensity as a function of θ



Resonant angle θ_r is a function of the dielectric constants of the two contacting media. Due to this property, the surface plasmon resonance can be utilized in monitoring surface reactions, as every new adlayer formed on the metal surface causes changes in dielectric function of medium ε_1 , establishing new resonance angle θ_r .

SPR curve measured for silver using Kretschmann Configuration

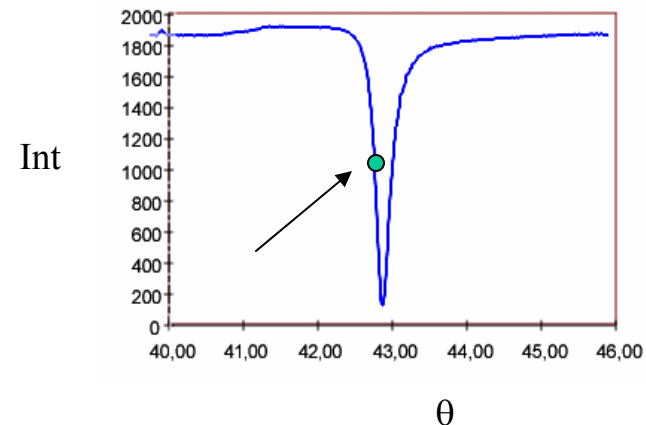
Fixed angle SPR detection



$\Delta n = 10^{-6}$ for sample exposed to air
 $\Delta n = 10^{-5}$ for liquid sample

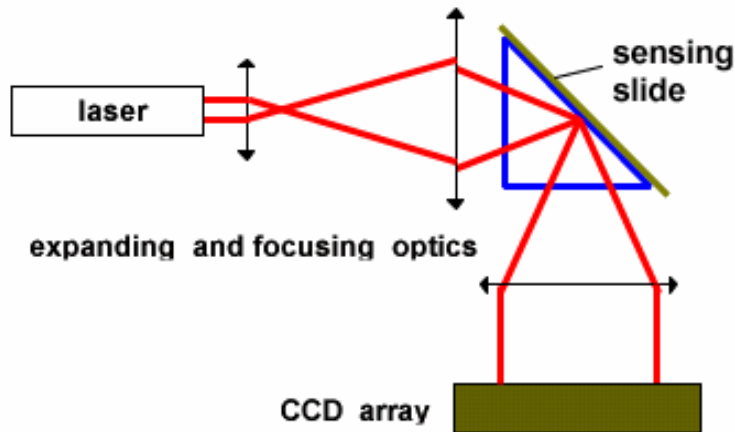
Optical sensitivity depends on metal used
 Noise suppression and light fluctuation compensation

- Using Kretschmann geometry measurement-
 - Recording whole resonance curve by turning the prism
 - Fixed angle when prism is stopped near its resonance dip.



The angle of incidence of light is fixed and chosen to be in the middle of the slope of the reflectance dip

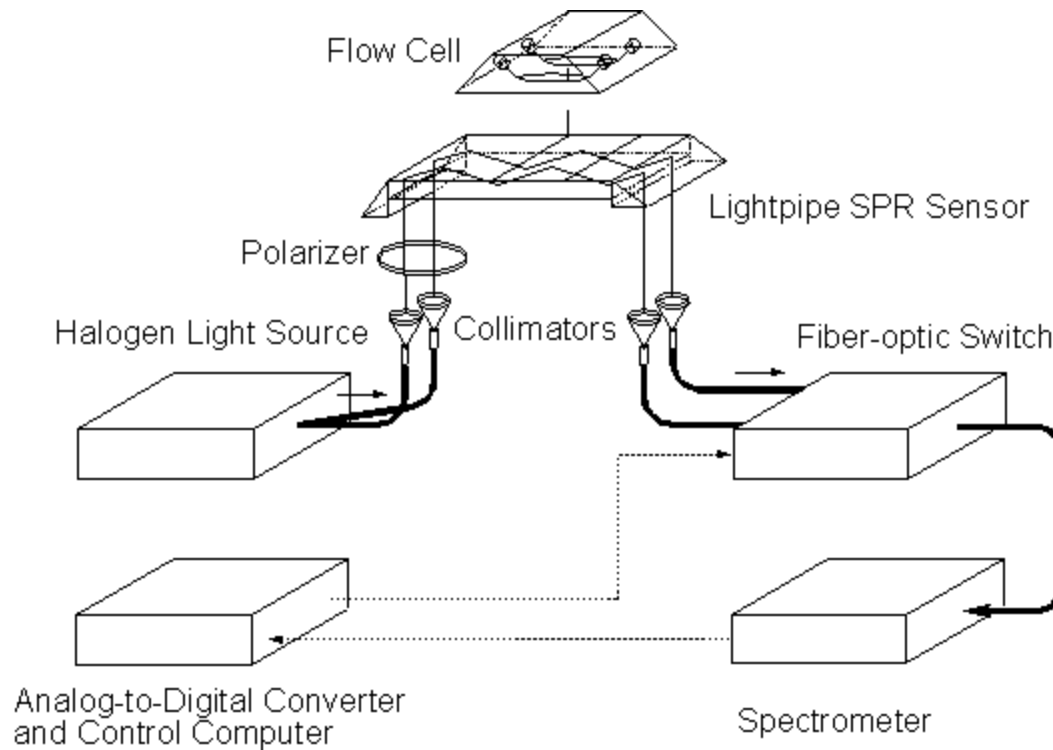
Focused Beam SPR detection



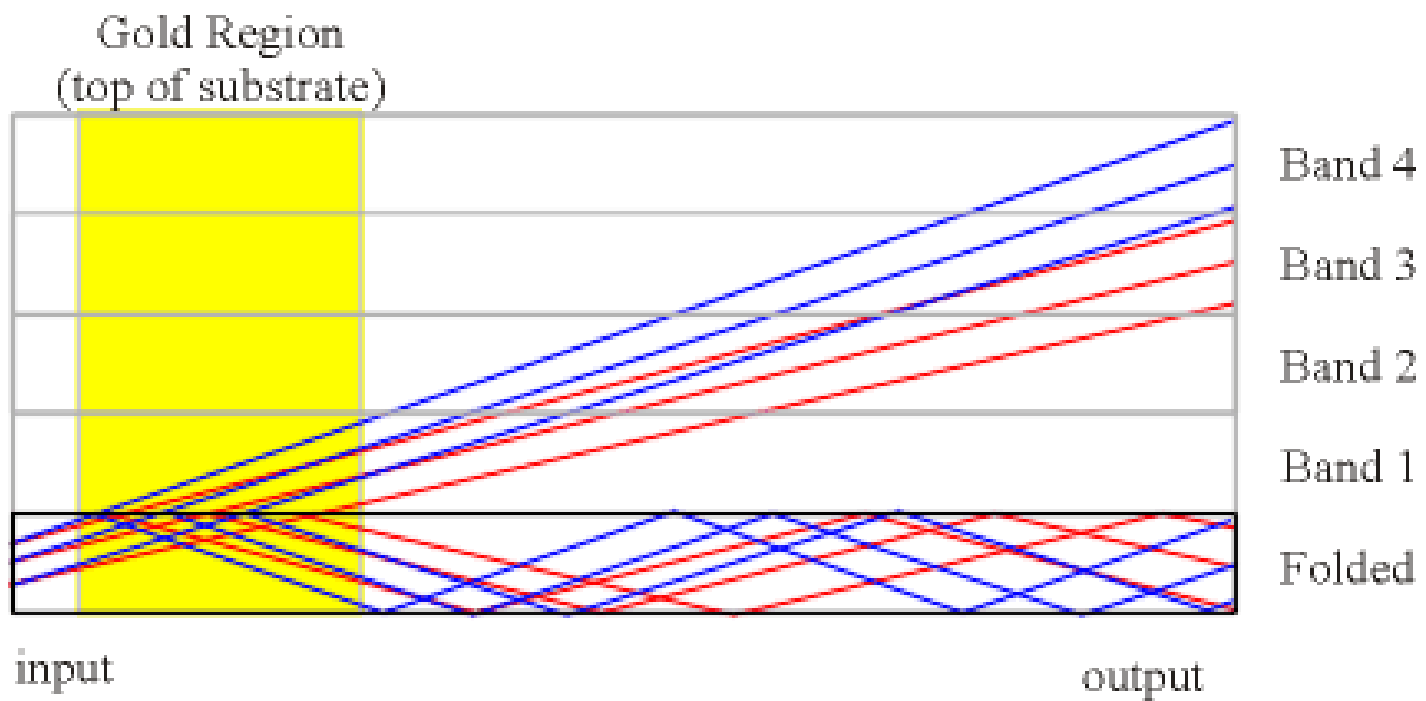
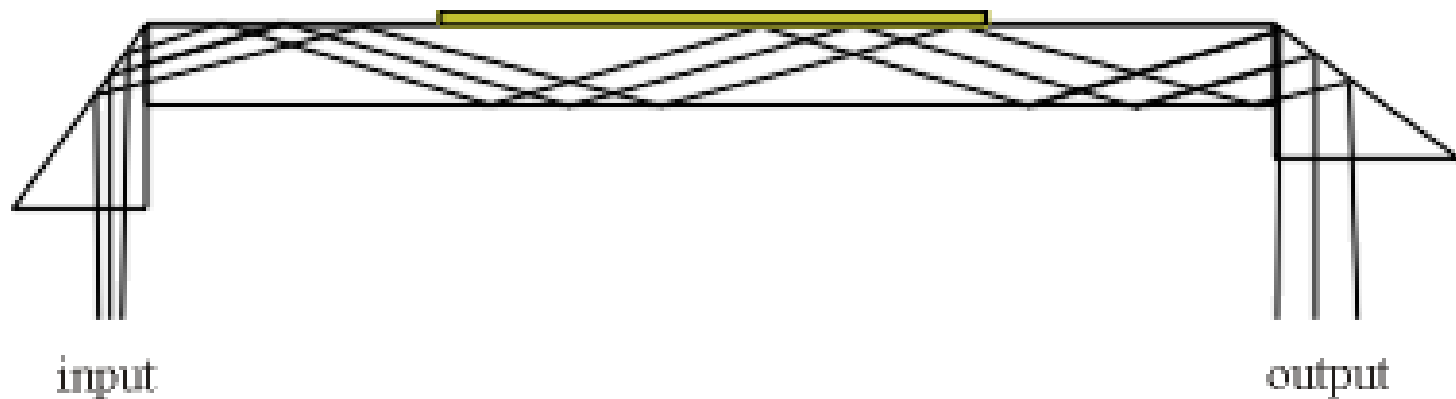
Idea of forming simultaneously more than one angle of incidence and thus being able to record the whole SPR curve without the necessity of rotating the prism.

The SPR curve and possible changes of its shape can be followed in real-time by a CCD array.

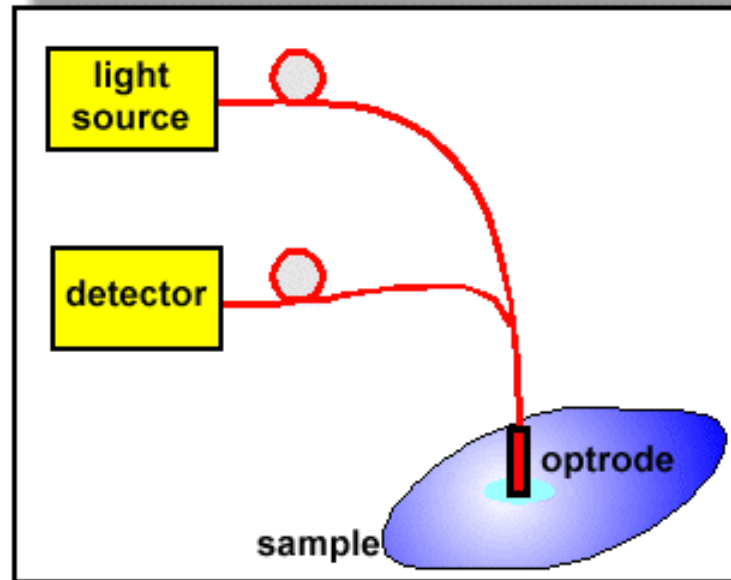
Commercial model of the focused SPR combined with multi channel flow cell system
With immunological studies are currently available on the market.



SPR lightpipe sensor developed at the University of Washington to detect biological toxins



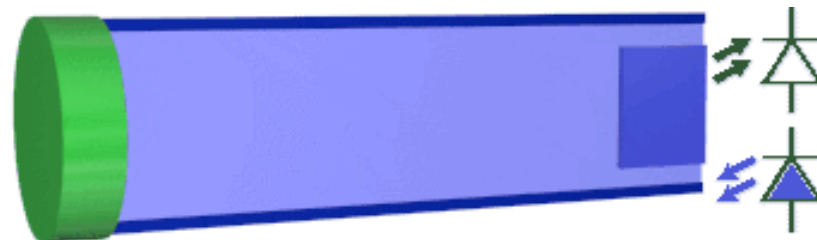
PH Sensor Operating Principle



The sensor consists of three main parts: light source, optrode and detector. The main part of the sensor, so-called optrode, contains an appropriate indicator which changes its optical properties in dependence on the analyte. In most cases, it is necessary to use an indicator because the analyte does not give or exhibit changes of optical properties. The indicator can change, for example, absorbance or fluorescence intensity. The light source is matched to the so-called analytical wavelength of the indicator then the best sensitivity of the sensor can be obtained. Detector, usually photodiode or PMT, converts optical signal into electric one which is next electronically processed.



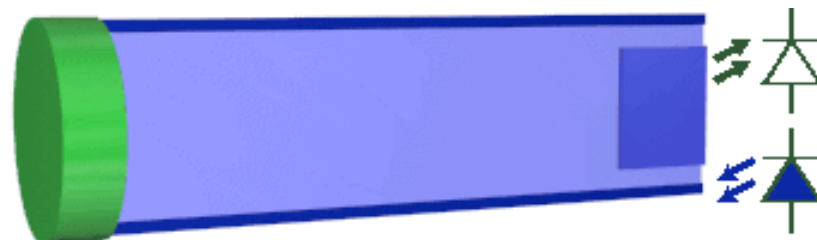
Operating principle of a pH sensor based on absorbance indicator



Sensor based on fluorescence indicator



Sensor based on absorbance indicator at solution of different pH



Sensor based on fluorescence indicator at solution of different pH

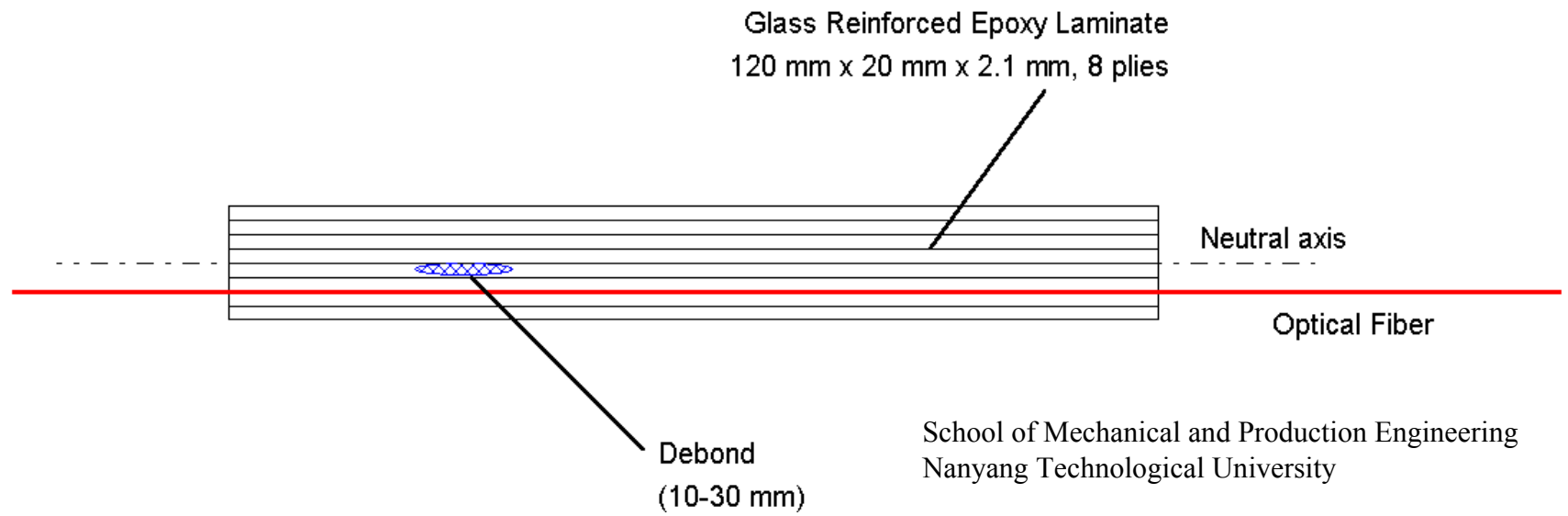
Smart Structure

Embedded Structure: concrete, metal, polymer, composite

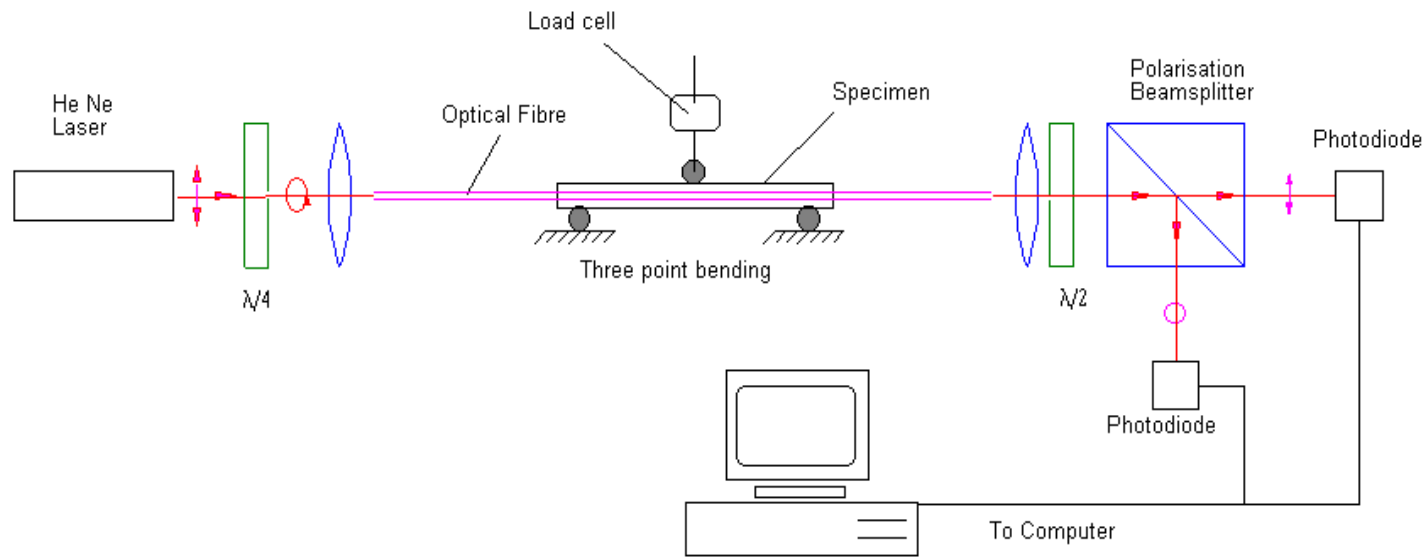
Applications: monitor and correct for structural changes in flight

Fiber reinforced polymer composites are becoming increasingly popular, damage detection in these materials has become an important issue.

Several schemes of damage detection using optical fiber sensors are being investigated



School of Mechanical and Production Engineering
Nanyang Technological University

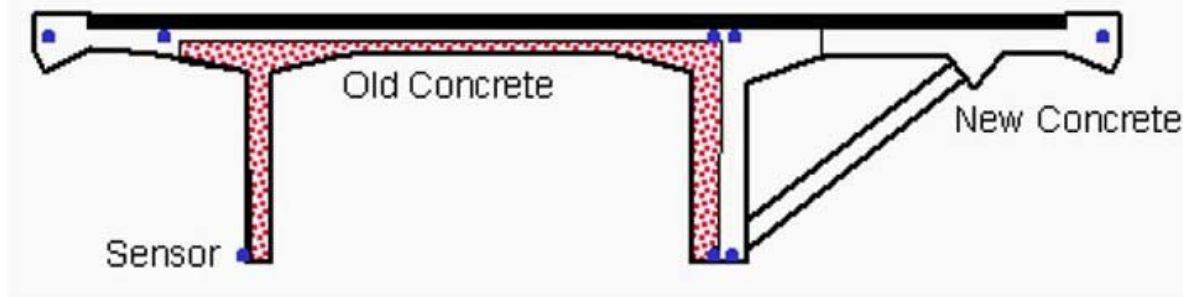


School of Mechanical and Production Engineering
Nanyang Technological University

Versoix bridge Project

Concrete monitoring during setting, old-new interaction evaluation, bending / torsion measurement, curvature analysis, long-term monitoring, automatic and remote monitoring, load testing, more than 100 fiber optic sensors installed

Versoix bridge Project



To monitor the behavior of the bridge during the works and in the long term, it was decided to instrument it with more than 100 sensors allowing the measurement of the curvatures at 13 different sections and the calculation of the bridge's horizontal and vertical deformations by double integration of the curvatures. Sensors pairs were also used to verify the adherence between old and new concrete.

Versoix bridge Project

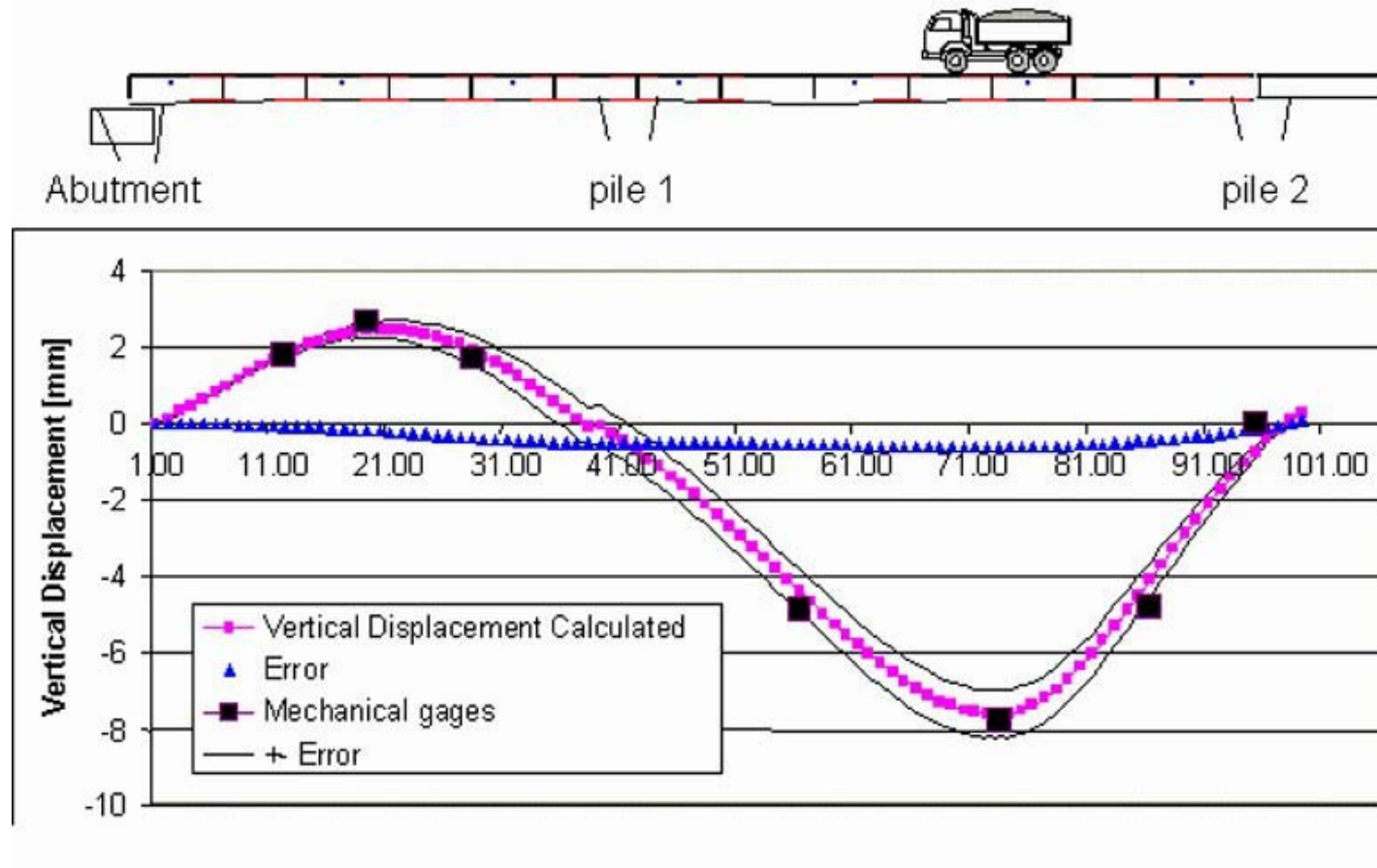
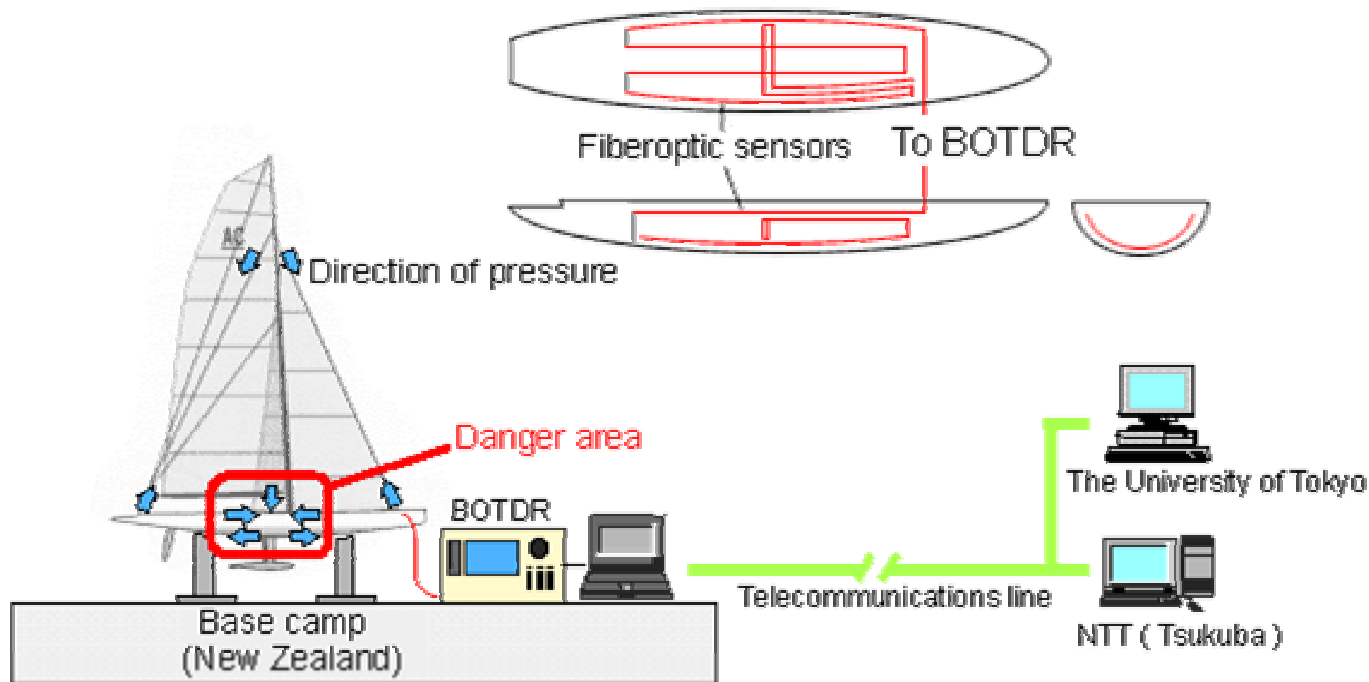


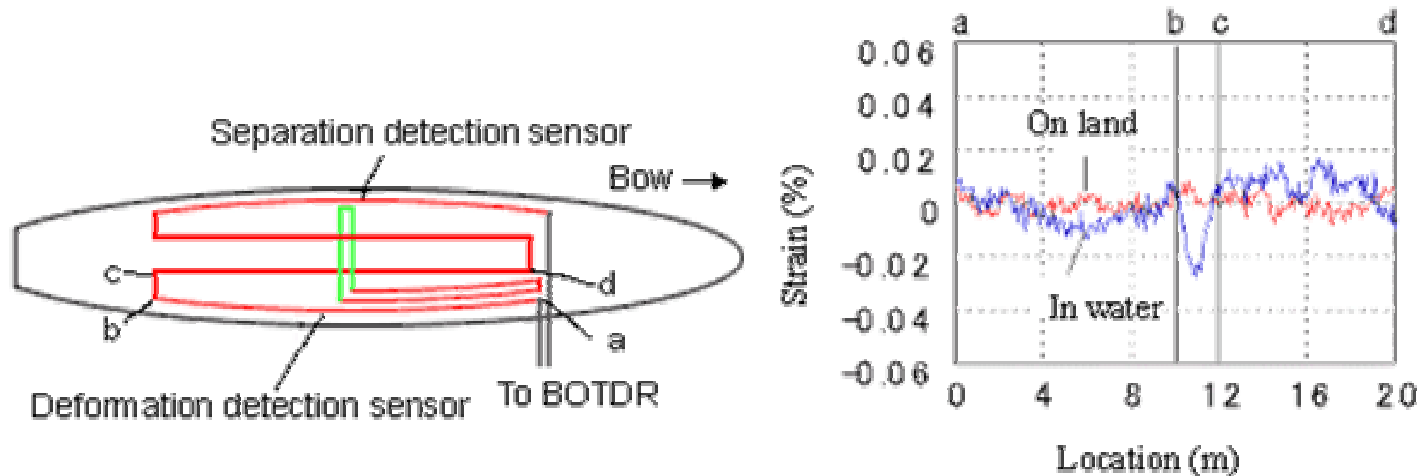
Image of the Fiberoptic Sensor Damage Detection System



Nippon Telegraph and Telephone Corp.
The University of Tokyo
GH Craft Ltd.

1) Feedback on hull structural design

This system produces three-dimensional strain data on the entire hull on the basis of the continuous strain measurement results by the fiberoptic sensors attached to the yacht rather than the point data by conventional sensors such as strain gauges[3]. Moreover, the system not only detects damage but allows checks on hull deformation.



2) Establishment of damage (cracks or debonding) detection methods

The point where cracks or debonding have actually occurred can be detected from the continuous strain distribution measured by the fiberoptic.

